Designing embedded retaining walls relying on the Generalized Coefficient of Earth Pressure and the elastic beam theory

Lysandros Pantelidis (lysandros.pantelidis@cut.ac.cy)
Cyprus University of Technology https://orcid.org/0000-0001-5979-6937

Research Article

Keywords: Intermediate earth pressure, the Generalized Coefficient of Earth Pressure, elastic beam theory, Eurocode 7, Eurocode 8-5

Posted Date: October 4th, 2022

DOI: https://doi.org/10.21203/rs.3.rs-2132476/v1

Designing embedded retaining walls relying on the Generalized Coefficient of Earth Pressure and the elastic beam theory

Lysandros Pantelidis[1,*]

[1] Cyprus University of Technology, 3036 Limassol, CY

* lysandros.pantelidis@cut.ac.cy

Abstract.

Intermediate values of earth pressure occur if the wall movements are insufficient to mobilize the active or passive limiting values. These values are of particular importance for designing embedded retaining walls, due to their flexible nature. The methods included in a standard are supposed to reflect the best (current) practice, however, the empirical methods included in EN1997-1:2004 and prEN1997-3:2022 are far from being considered reliable. Very recently, the author proposed a continuum mechanics approach for deriving earth pressure coefficients for any soil state between the at-rest state and the active or passive state, applicable to cohesive-frictional soils and both horizontal and vertical pseudo-static conditions. The same method also provides analytical expression for the calculation of the required wall movement (at any depth) for the mobilization of the active or passive failure state. In the present paper the author suggests a new, fully analytical method for designing embedded retaining walls, combining the aforementioned method with the well-known elastic beam theory. An application example is given indicating remarkable agreement with the finite element method, while when the proposed method is followed, more stable results are returned.

Keywords: Intermediate earth pressure, the Generalized Coefficient of Earth Pressure, elastic beam theory, Eurocode 7, Eurocode 8-5

1 Introduction

Intermediate values of earth pressure occur if the wall movements are insufficient to mobilize the active or passive limiting values. These values are of particular importance for designing embedded retaining walls, due to their flexible nature. The methods included in a standard are supposed to reflect the best (current) practice; thus, in this paper, the author will focus on

what EN1997-1:2004 [1] and prEN1997-3:2022 [2] (draft standard) foresee. More specifically, both EN1997-1:2004 and prEN1997-3:2022 suggest that intermediate values of earth pressures be calculated using empirical rules, beam on springs models, or continuum numerical models. Such empirical rules are included in Annex C (denoted as informative) of EN1997-1:2004. According to this annex, intermediate values of active earth pressure between the at-rest state and the limit state may be obtained by linear interpolation, while intermediate values of passive earth pressure between the at-rest state and the limit state may be obtained by parabolic interpolation. The latter is materialized using an empirical parabolic relationship (see Figure C.3 of EN1997-1:2004), which, however, stands only for non-cohesive soils, while it relies on approximate values for wall movement for mobilizing the active or passive state (given in Table C.2 of EN1997-1:2004 in non-dimensional form).

prEN1997-3:2022 (Annex D denoted also as informative), on the other hand gives some guidance related to the application of a) beam-on-spring models based on the subgrade reaction coefficient, k, and b) an empirical interpolation function between the passive and the at-rest coefficients. For numerical continuum models (see Annex D11 in prEN1997-3:2022) only mentions that "in the case of retaining structures, only non-linear models provide relevant information with respect to both horizontal and vertical displacements within the ground mass".

Regarding beam-on-spring models prEN1997-3:2022 suggests that k be approximated by the empirical ratio of the secant soil's modulus of elasticity (E_s) over the interaction length (d). Some also empirical rules are given for the determination of both E_s and d, e.g., d must be less than $2/3D$, where D is the embedment depth and E_s has a value between the initial loading modulus and the unload-reload modulus. These rules are, however, very ambiguous, strongly subjected to subjective engineering judgement. Indeed, prEN1997-3:2022 itself notes that this is a simplification that assimilates the ground to independent springs and that due to its empirical nature, values of the coefficient of subgrade reaction should always be determined from comparable experience in similar conditions. Moreover, it mentions that spring stiffness values are very software specific.

As an alternative method, the intermediate passive earth pressure coefficient (called horizontal component of the mobilized passive earth pressure coefficient by prEN1997-3:2022) is calculated using the following empirical interpolation function between the coefficient of earth

pressure at rest (K_{O}) and the horizontal component of the coefficient of passive earth pressure (K_{ph}):

$$K_{\mathrm{ph,mob}}(z) = K_{\mathrm{O}} + \left(K_{\mathrm{ph}} - K_{\mathrm{O}}\right)\frac{v(z)/z}{a_b + v(z)/z} \quad (1)$$

where, z is the depth, $v(z)$ is the horizontal displacement at depth z and a_b is an empirical backfill-dependent coefficient (in the absence of detailed specifications, it is suggested that a be taken equal to 0.02). For a rigid wall rotating about its base prEN1997-3:2022 suggests that $v(z) = s_h(1 - z/h)$, with s_h being the horizontal displacement at the wall top and h is the height of the retaining wall. Apparently, Equation 1 has no value once $v(z)$ is unknown, thus, its applicability is restricted to rigid walls rotating about their base. It seems that prEN1997-3:2022 has abandoned the empirical interpolation functions of its predecessor, which have now been replaced by a unique but also empirical formula (Equation 1).

Apparently the simplistic and empirical nature of the above approaches raise serious queries about their validity. Thus, it seems that among the above, the best option is the numerical modelling. It is finally very interesting that neither EN1998-5:2004 nor prEN1998-5:2022 deals with intermediate earth pressures (they deal with only the earth pressures at-rest and the two limit states). Intermediate earth pressure is a very challenging problem and any approach, other than the numerical one, should be proposed on a stable basis and supported by relevant documentation. In this respect, the author [3] proposed in 2019 a continuum mechanics approach for deriving earth pressure coefficients for any soil state between the at-rest state and the active or passive state, applicable to cohesive-frictional soils and both horizontal and vertical pseudo-static conditions. The same method also provides analytical expression for the calculation of the required wall movement Δx_{max} for the mobilization of the active or passive failure state. The basic expressions are summarized in the following section, while the proposed approach for designing embedded retaining walls combines these expressions with the elastic beam theory.

2 The Generalized Coefficient of Earth Pressure

The generalized coefficient of earth pressure for cohesive – frictional soils, being at any state X is given by the following equation:

$$K_{XE} = \frac{1-(2\lambda-1)\sin\varphi_m}{1+(2\lambda-1)\sin\varphi_m} - (2\lambda-1)\frac{2c_m}{(1-a_v)(\sigma_v-u)}\tan\left(45^o - (2\lambda-1)\frac{\varphi_m}{2}\right) \quad (2)$$

where, c_m and φ_m are the mobilized shear strength parameters of soil, a_v is the vertical pseudo-static coefficient, u is the pore water pressure and σ_v is the vertical total stress. λ is a soil state dependent coefficient being either 0 or 1. X is O, A, P, IA or IP denoting the at-rest, active, passive, intermediate active and intermediate passive state respectively. This is the same expression given earlier by the author [3], but here it is given in a more elegant and general form, rather reminding of Rankine's [4] equation.

The mobilized cohesion of soil, c_m, is calculated using Equation 2.

$$c_m = c'\frac{\tan\varphi_m}{\tan\varphi'} \quad (3)$$

The mobilized internal friction angle of soil, φ_m, derives from the solution of Equation 3.

$$\sin\varphi_m\left(C_1 - (2\lambda-1)B_1\frac{\tan\varphi_m}{\tan\varphi'}\right) = \left|1 - A_0 + (2\lambda-1)B_1\frac{\tan\varphi_m}{\tan\varphi'}\right| \quad (4)$$

The analytical solution of Equation 3 is given in Appendix A, while φ_m is also given in chart form in Pantelidis [3]. The parameters C_1, B_1, A_0 and λ are also defined in Appendix A.

For purely frictional soils, Equation 1 takes the following convenient form for each soil state X, that is, without the need for calculating φ_m:

$$K_{AE} = \frac{1-\sin\varphi'}{1+\sin\varphi'}\left(1 + 2\cdot\tan\theta_{eq}\cdot\tan\varphi'\right) \quad (5)$$

$$K_{IAE} = \frac{1-\sin\varphi'}{1+\sin\varphi'}\left((1-\xi\cdot\sin\varphi') + \tan\theta_{eq}\cdot\tan\varphi'\left(2+\xi\cdot(1-\sin\varphi')\right)\right) \quad (6)$$

$$K_{OE} = (1-\sin\varphi')\left(1+\tan\theta_{eq}\cdot\tan\varphi'\right) \quad (7)$$

$$K_{IPE} = \left(\frac{1+\sin\varphi'}{1-\sin\varphi'}\right)^{\xi_1}\left((1+\xi\cdot\sin\varphi') + \xi_2\cdot\tan\theta_{eq}\cdot\tan\varphi'\left(2+\xi\cdot(1+\sin\varphi')\right)\right) \quad (8)$$

$$K_{PE} = \frac{1+\sin\varphi'}{1-\sin\varphi'}\left(1 - 2\cdot\tan\theta_{eq}\cdot\tan\varphi'\right) \quad (9)$$

where, $\theta_{eq} = atan\left(\frac{a_H}{1-a_V}\right)$ in the absence of pore water pressure or $\theta_{eq} = atan\left(\frac{a_H}{1-a_V}\frac{\sigma_v}{\sigma_v-u}\right)$ in the presence of pore water pressure, while $\xi_1 = 1+\xi$, $\xi_2 = 2/m-1$ and $\xi = (m-1)/(m+1)-1$.

m is a real positive number (ranging from 1 to $+\infty$) calculated as follows:

$$m = \left(1+\frac{\Delta x}{\Delta x_M}\left(\frac{H}{z}\right)^{1+\frac{\Delta x}{\Delta x_M}}\right)\left(1-\frac{\Delta x}{\Delta x_M}\right)^{-1} \quad (10)$$

ξ_1 and ξ_2 are parameters related to the transition from the soil wedge of the state at-rest to the soil wedge of the passive state. m, in essence, defines all intermediate states between the active (or passive) failure state; the effectiveness of this parameter is shown in Appendix B.

Δx_M is the required horizontal displacement for the development of the active or passive state at the mid-height of the retained soil. That is, $\Delta x_M = \Delta x_{max}(z/H{=}0.5)$; since H is different for the two sides of the wall (H_A and H_P for the active or the passive "side" of the problem respectively), Δx_M has different value for each side of the wall. z, here, is a general symbol for indicating depth on the active or the passive "side" (z_A and z_P respectively). For $0 \le z/H \le 0.5$, Δx_{max} is calculated using Equation 10 for smooth (unfavorable case) retaining walls. For $0.5 \le z/H \le 1$, the value of Δx_{max} is equal to the one corresponding to $z/H = 0.5$.

$$\Delta x_{max} = \frac{\pi}{4}\frac{(1-\nu^2)}{E}\frac{(1+z/H)^3(1-z/H)}{z/H}H\cdot\Delta K\cdot(1-a_v)(\sigma_v-u) \quad (11)$$

$\Delta K = K_{OE} - K_{AE}$ or $K_{PE} - K_{OE}$, depending on the case examined while E and ν are the elastic modulus and Poisson's ratio of the retained soil. Δx_{max} becomes maximum for z/H=0.5.

Δx is the deflection of the wall at depth z calculated based on the theory of elastic beams (e.g., cantilever beam for cantilever wall and simply supported beam for propped cantilever wall). For the authors' convenience, the basic elastic beam theory equations for calculating Δx for the case of cantilever beam with partially distributed linearly varying load (trapezoidal) are given in Appendix C.

The total earth pressure at depth z_A (or z_P) acting perpendicular to a vertical or nearly vertical retaining structure for any soil state X, therefore, is

$$\sigma_{XE} = K_{XE}(1 - a_v)(\sigma_v - u) + u \quad (12)$$

The resultant earth pressure force derives from the σ_{XE} - z chart area:

$$P_{XE} = \int_H^0 \sigma_{XE} dz \quad (13)$$

H is either the height of the retained soil on the active or the passive "side" of the problem (H_A and H_P respectively).

It is important to be mentioned that both the proposed earth pressure coefficients and the expression for Δx_{max}, are accompanied by an exhaustive validation procedure and comparison with the earth pressure methods included in EN1998-5:2004 [5], prEN1998-5:2022 [6] and AASHTO [7] standards (see [8]). The comparison includes among others, centrifuge test results from two different studies, and results from 157 finite element models from two different programs. In addition to this, based on the proposed coefficient or earth pressure at-rest, the author [9] offered an analytical method for the calculation of the shaft resistance capacity of axially loaded piles in cohesive-frictional soils under static or pseudo-static conditions based on ground parameters. With the results being extremely close to those obtained by the finite element method, this may also be regarded as validation of the author's Generalized Coefficient of Earth Pressure.

3 Application of the proposed analytical procedure and comparison with the finite element method

The analysis that follows combines the earth pressure method proposed by the author [3] and the elastic beam theory. The procedure is described in detail through an application example, the data of which are listed in Figure 1. The example in question has been solved twice for comparison purposes, first with the proposed analytical procedure (using an MS Office Excel spreadsheet) and later with the finite element method (using Rocscience's RS2).

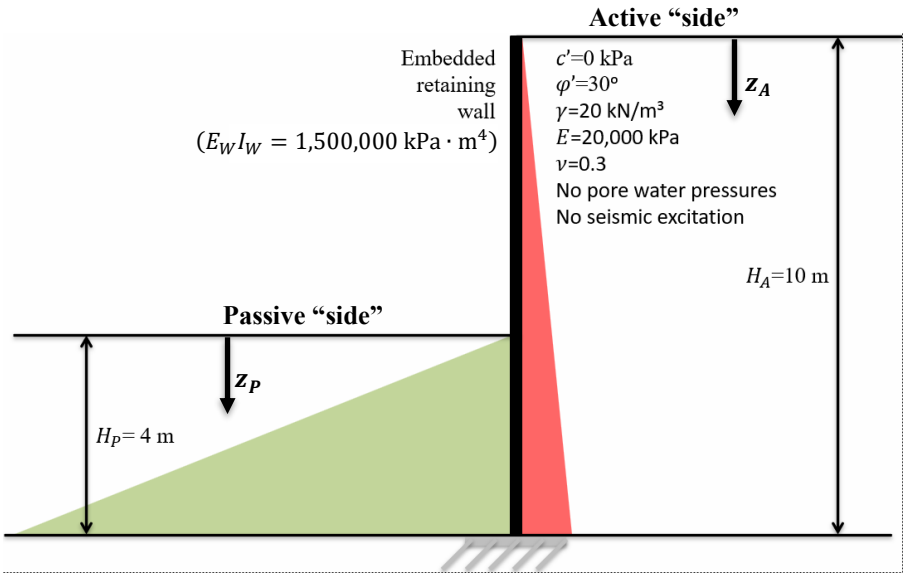

Figure 1. Data for the application example.

Regarding the proposed analytical procedure, the deflection Δx at any depth z is calculated based on the elastic beam theory, where the embedded wall of Figure 1 is treated as a cantilever beam (see Appendix C; a propped retaining structure is treated accordingly); the earth pressures on the two sides of the wall constitute the loading acting on the beam, where the principle of superposition stands. An iterative procedure is needed; this is presented step by step in Appendix D. As a starting point (1st iteration; see Table A1 in Appendix D), it is logical and convenient to assume that the soil on both sides of the wall is at the state at-rest (that is, Δx=0 m, meaning that Equation 1 is applied for $m = 1$; recall Equation 9). However, since $H_A > H_P$, this state, cannot be true (at least for the majority of points along the wall); the embedded wall will have the tendency to bend towards the passive "side" (although this is controlled by the flexural rigidity of the wall). The deflection of the wall caused by the combined action of the earth pressure distributions acting on the two sides of the wall is then calculated; these deflection values are denoted by the symbol Δx_{tot} (Δx value for the active case minus the respective Δx for the passive case; see Table A1 in Appendix D). These Δx_{tot} values are then copied to the two Δx columns of the 2nd iteration (see Table A2 in Appendix D), constituting the new data set and so on, until convergence to be achieved. As shown, the five iterations considered

178 in the present example were adequate for obtaining stable results (see Tables A1-A5 in Appen-
179 dix D). The final results, as these have been obtained in the last (5th) iteration and corrected
180 (when necessary) are shown in Table 1. Correction is necessary when $\Delta x_{tot} > \Delta x_{max}$; this
181 inequality indicates that the soil has reached its failure state.
182

183 *Table 1. Final results, as these have been obtained in the last (5th) iteration and corrected (when necessary; i.e. when*
184 *$\Delta x_{tot} > \Delta x_{max}$).*

Active "side"						Passive "side"					
$z_A = z$ (m)	Δx_{max} (mm)	Δx_{tot} (mm)	φ_m (°)	K_{XE}	σ_{XE} (kPa)	z_P (m)	Δx_{max} (mm)	Δx_{tot} (mm)	φ_m (°)	K_{XE}	σ_{XE} (kPa)
0	11.9	17.03	30.00(1)	0.333(1)	0.00						
0.5	13.1	15.97	30.00(1)	0.333(1)	3.33						
1	14.3	14.92	30.00(1)	0.333(1)	6.66						
1.5	15.4	13.86	29.581	0.339	10.17						
2	16.5	12.80	29.130	0.345	13.81						
2.5	17.4	11.75	28.487	0.354	17.71						
3	18.3	10.70	27.678	0.366	21.94						
3.5	19.1	9.65	26.757	0.379	26.54						
4	19.6	8.61	25.785	0.394	31.50						
4.5	20.0	7.59	24.819	0.409	36.78						
5	20.1	6.58	23.902	0.423	42.33						
5.5	20.1	5.60	23.061	0.437	48.08						
6	20.1	4.65	22.307	0.450	53.97	0	28.6	4.65	12.214	0.348	0.00
6.5	20.1	3.74	21.646	0.461	59.94	0.5	35.6	3.74	2.679	0.911	9.11
7	20.1	2.90	21.077	0.471	65.94	1	41.9	2.90	11.296	0.672	13.45
7.5	20.1	2.12	20.597	0.480	71.93	1.5	46.5	2.12	14.958	0.590	17.69
8	20.1	1.44	20.203	0.487	77.86	2	48.2	1.44	16.951	0.548	21.94
8.5	20.1	0.86	19.892	0.492	83.68	2.5	48.2	0.86	18.162	0.525	26.24
9	20.1	0.41	19.665	0.496	89.35	3	48.2	0.41	18.911	0.510	30.63
9.5	20.1	0.11	19.522	0.499	94.82	3.5	48.2	0.11	19.332	0.503	35.18
10	20.1	0.00	19.471	0.500	100.00	4	48.2	0.00	19.471	0.500	40.00

185 (1) Corrected values
186

187 It is reminded that the procedure in Appendix D considers only bending of the wall (that is,
188 the lower end of the wall is considered to be fixed; typical case of cantilever beam). However,

189 in addition to bending, the actual deformation may involve translation and/or rotation; this is
190 discussed later in the present work.

191 The same problem was solved again, this time numerically using Rocscience's RS2; RS2 is
192 a commercial program for 2D finite element analysis of geotechnical structures for civil and
193 mining applications. The geometry, mesh and boundary conditions in this plane strain problem
194 are shown in Figure 2. Favoring reproduction of the example problem, all relevant information
195 is given below (if something is not mentioned, the RS2 default value was used). The "Gaussian
196 elimination" solver type was used. Regarding the "stress analysis" menu, the maximum number
197 of iterations was 1000, the tolerance was set to 0.001, while the "comprehensive" convergence
198 type was adopted (the "comprehensive" setting means that force, energy, and displacement is
199 checked at the same time). The "mesh type" was set to "graded", while 6-noded triangular
200 elements were used (meaning, in this respect, 19.0 nodes/m^2 or 9.2 elements/m^2; see Figure 2).
201 The wall was extended five meters below the lower end shown in Figure 1 for producing the
202 fixed "beam" conditions in the finite element analysis (see Figure 2). The author noticed that
203 more stable results are returned when a very small horizontal nodal displacement (1/10 mm to
204 the left) is given to the extra wall length, instead of embedding the latter in a different, much
205 stiffer material. The author also noticed that the same nodal displacement but to the right, does
206 not affect the results. In addition to the above, the "field stress type" was "gravity" with "stress
207 ratio" in- and out-of-plane equal to 0.5 (recall Equation 6 for φ'=30^o and θ_{eq}=0). The "initial
208 element loading" was "field stress and body force". The problem was solved statically (θ_{eq}=0).
209 The soil parameters were those given in Figure 1 (apparently, the "plastic" material type was
210 chosen). The wall (with its extra length for embedment) was modeled as "structural interface",
211 with a "standard beam" element as liner (core) and a "joint" element at both sides (crust). The
212 liner was considered to be "elastic" with Young's modulus E_w=15·10^6 kPa and thickness
213 1.0627 m (moment of inertia I_w=1.0627^3·1/12=0.1 m^4); this combination of values gives the
214 E_wI_w=1.5·10^6 kPa·m^4 (beam stiffness) value used by the author in the analytical solution (the
215 Poisson's ratio of the liner was 0.01, while the "Timoshenko" beam element formulation was
216 adopted). Regarding "joint", the "material dependent" slip criterion was chosen with "interface
217 coefficient" as low as 0.05 (it is reminded that the proposed earth pressure analysis method is
218 for smooth walls; the roughness of the wall is also discussed later). Both the normal and shear

stiffness of the joint element was set to 200.000 kPa/m. In this respect, Rocscience [10] suggests as "a good place to start" a normal joint stiffness approximately 10 times the minimum modulus of the two materials on each side of the joint and a shear stiffness approximately the same as the minimum modulus. According again to Rocscience, this generally gives results that are fairly insensitive to the stiffness values.

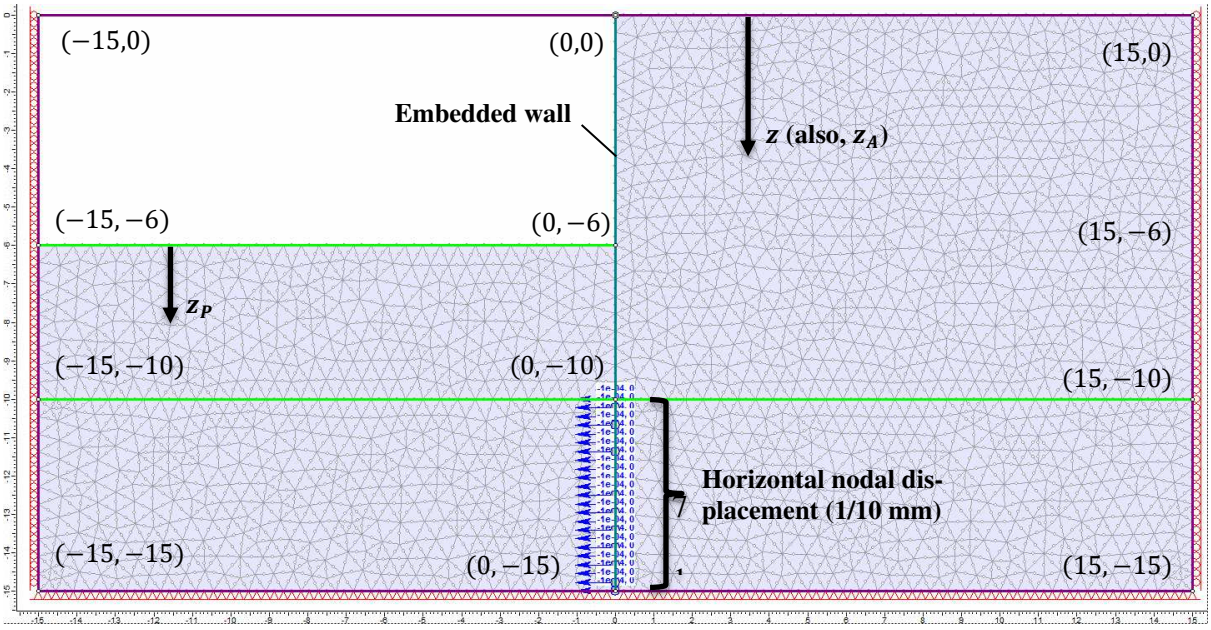

Figure 2. Geometry, mesh and boundary conditions of the example problem considered in Rocscisnce's RS2.

In the chart of Figure 3 the analytically and numerically derived deflection values of the wall have been drawn against depth; the $\Delta x_{max,A}$ and $\Delta x_{max,P}$ values (for the active and passive state respectively) are also shown on the same chart. In this respect, a number of onservations can be made: a) the proposed method effectively calculated the deflection of the embedded wall, b) an active failure state zone exists near the top of the wall ($\Delta x_{tot} \geq \Delta x_{max,A}$), while for the rest of the soil mass adjacent to the wall, the soil is at an intermediate active or passive state, c) there is a strange abnormality in the finite element analysis curve at z=10 m (depth of fixed point of the wall), where the wall seems to be broken (but is does not, because it is of an elastic material) and e) the analytical solution shows that the soil in the passive "side" of the problem is far from failure; besides, a deflection as low as 4.5 mm (maximum deflection,

238 referring to z_P=0 m) is not able to cause a passive failure in the spesific soil, not even an active
239 one (see Figure 3).
240

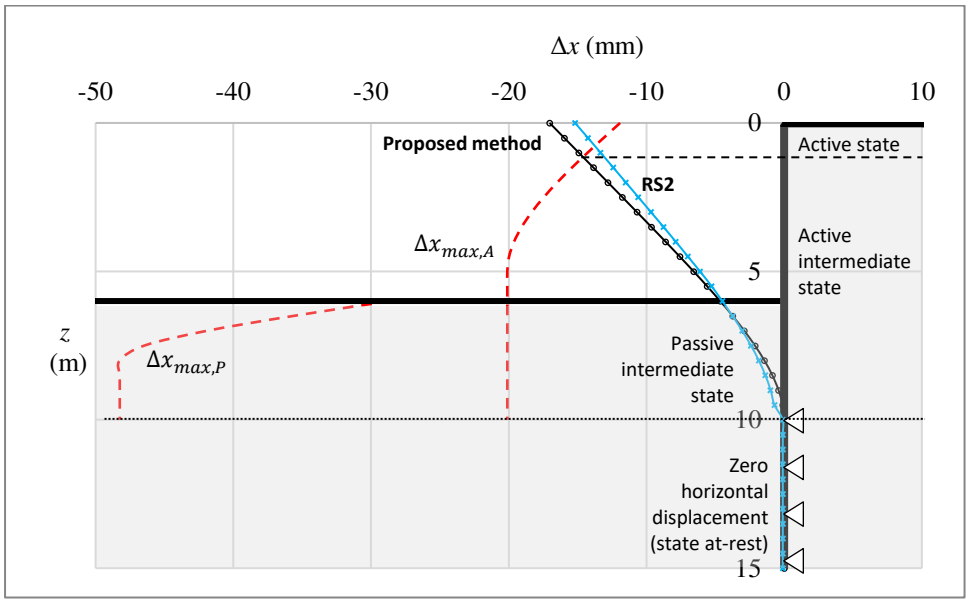

241
242 *Figure 3. Deflection off embedded wall versus depth chart.*

243 The analytical and numerical earth pressure distributions have been drawn against depth in
244 Figure 4. As shown, the two "active" curves (the analytical and the numerical ones) coincide
245 quite well, with the numerical curve just to indicate a deeper active failure zone. Also, as ex-
246 pected, for z>10 m (that is, for z below the theoretical fixed point of the wall), both curves
247 coincide with the theoretical earth pressure at-rest distribution; there is only a rather minor
248 abnormality around the z=10 m point, but this is something rather usual in a finite element
249 analysis when there is an abrupt change in the model. For the passive state the analytical curve
250 shows earth pressures closer to the respective earth pressures at-rest, something that can be
251 justified by the small deflection values with respect to the respective $\Delta x_{max,P}$ threshold values.
252 The "passive" numerical curve, on the other hand, shows a very peculiar behavior with great
253 intermediate earth pressure values which, indeed, for $6\,m < z < 7\,m$ are extremely close to
254 the passive state ones. In addition, for z>10 m, where the wall has been held practically still,
255 the numerical earth pressures are (much) greater than the logically expected earth pressures at-
256 rest. The negative values in Figure 4 just indicate the passive "side"; apparently the earth pres-
257 sure at-rest values obtained at the active "side" should also stand for the passive "side".

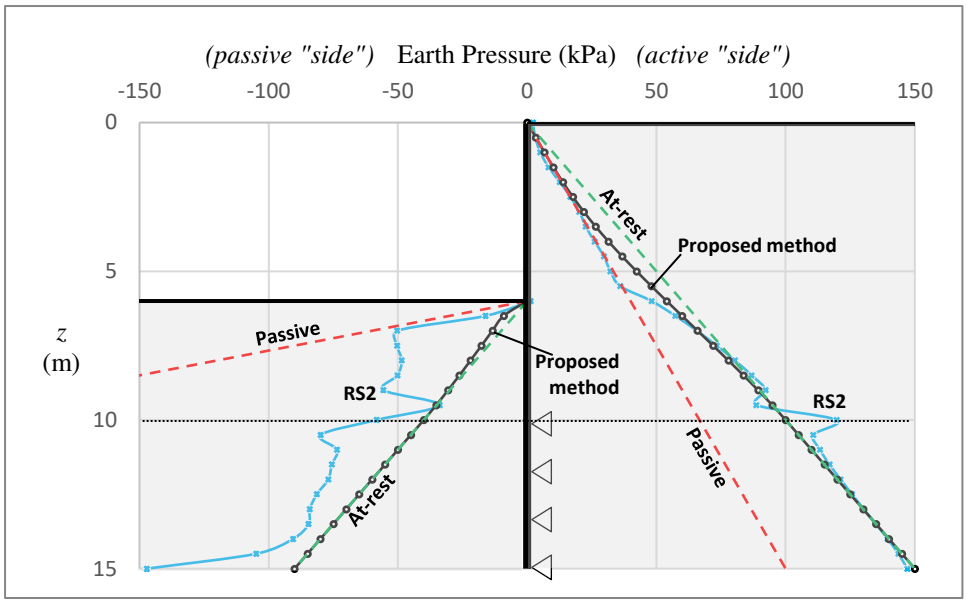

Figure 4. Chart showing the earth pressures on both sides of the embedded wall, as these have been calculated analytically using the proposed method and numerically using RS2. The "active", "passive" and "at-rest" lines show the threshold values.

The strange abnormality in the numerical deflection curve of Figure 3 for z=10 m indicate wall rotation (that is, there is a pivot point at z=10 m). The rotation was calculated equal to just 0.00688°. Applying the rotation in question to the analytical solution, the analytical curve almost overlaps with the respective numerical one for the active "side" of the problem (see Figure 5). Regarding the passive "side", greater intermediate passive earth pressure values were obtained, as expected, but not the peculiar and definitely not correct numerical values.

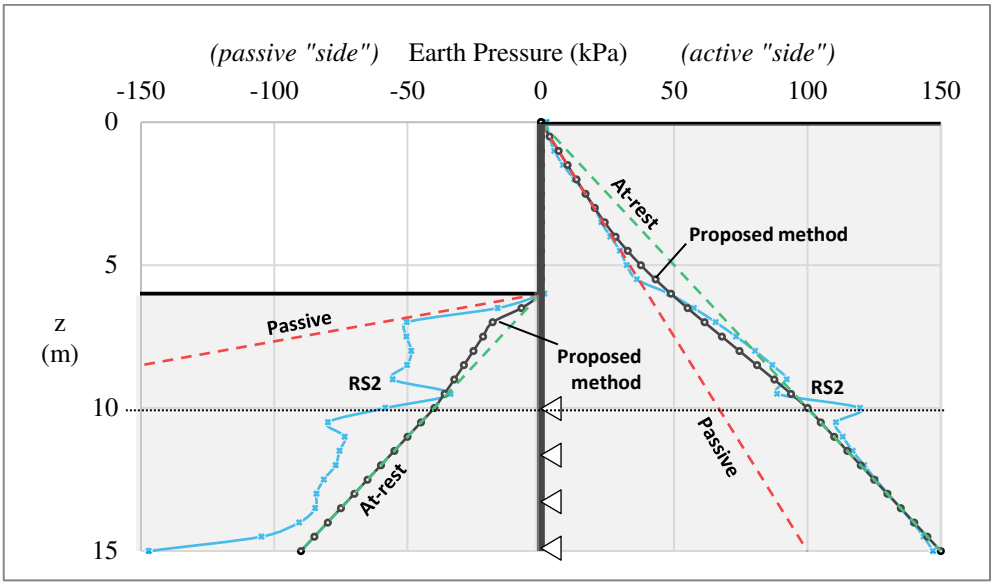

Figure 5. Same as Figure 4, instead of the fact that rotation equal to 0.00688º degrees as for the z=10 m point (towards the passive "side") was applied in the proposed analytical solution.

However, any embedded retaining wall, in addition to bending, may be rotated (around a pivot point being between its lower end and the free-soil surface on the passive "side") and/or be translated horizontally. The wall, which floats in the soil, will find its final position satisfying simultaneously: a) the *equilibrium of the energy* (herein, this is quantified by the work done by the earth pressures on the two sides of the wall) and b) the *principle of least action* (saying that, in some sense, the true motion is the optimum out of all possible motions). Applying different horizontal translational movements to the wall (in addition to bending), the work done against the uniform horizontal translation of wall chart of Figure 6 was obtained. The latter, indicates a required translational movement for the embedded retaining wall equal to 1.242 mm. Relatively, the earth pressure and deflection charts are given in Figures 7 and 8 respectively. Apparently, the curves in these charts will differ more or less if the wall is able to rotate; however, rotation requires optimization with two additional factors, the location of the pivot point and the angle of rotation. The work done by a force is simply calculated by the product of the force and the displacement that this force caused to the object. In this respect, the wall has been divided into segments of 0.5 m. The chart area between the earth pressure distribution and the z-axis for a specific wall segment gives the respective resultant force, while the average

deflection along this segment gives the required displacement for the calculation of the work done. Summarizing, the total work done on the active "side" must be equal to the total work done on the passive "side", while these works must be the least possible.

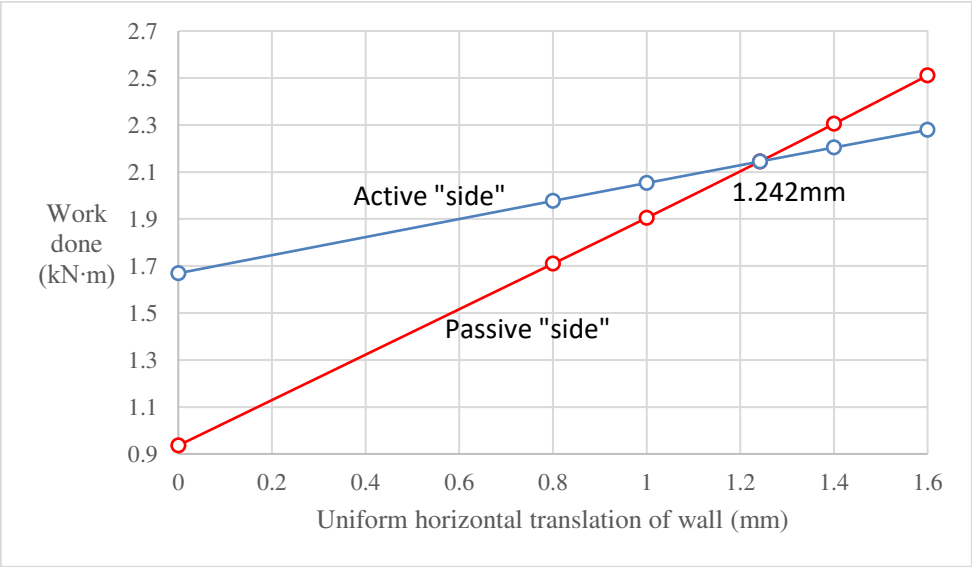

Figure 6. Work done against uniform horizontal translation of wall chart.

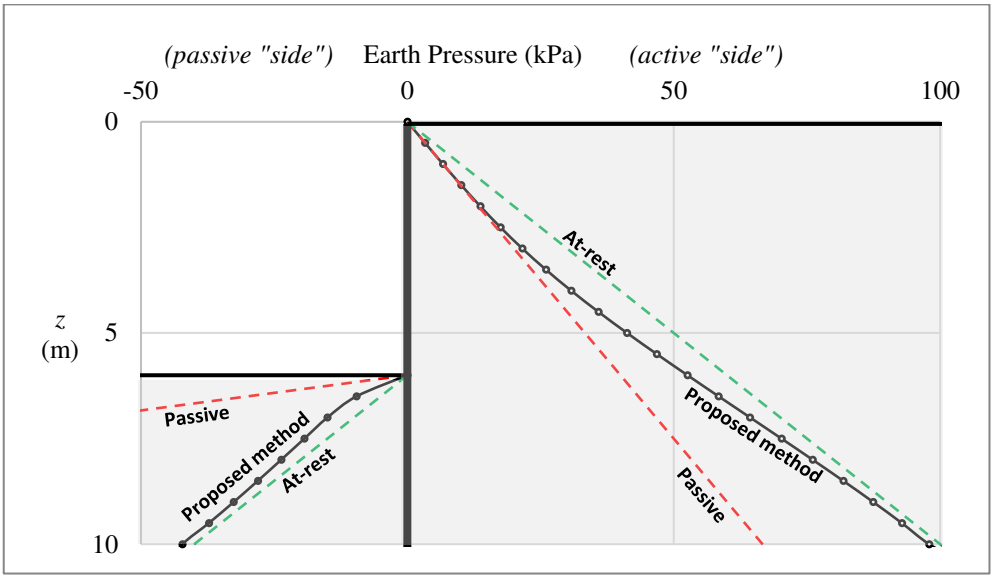

Figure 7. Earth pressure versus depth chart for the case where the work done on both sides of the wall are equal each other ("bending + 1.242 mm horizontal translation" case). No wall rotation was allowed.

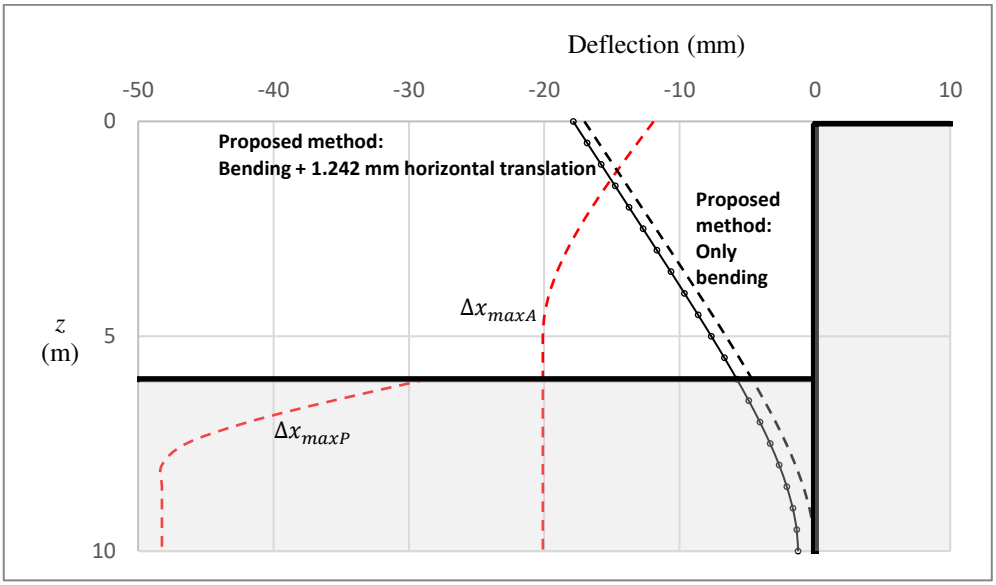

Figure 8. Deflection versus depth chart for "only bending" and "bending + 1.242 mm horizontal translation" cases.

The moments and shear forces along the wall were calculated and drawn in Figure 9 for the "only bending" case. Also, since both the deflection and the final intermediate earth pressure values are known, the modulus of subgrade reaction (k) values can easily be calculated by the stress over deflection ratio. These values are shown in Figure 10 both for the "only bending" and the "bending + 1.242 mm horizontal translation" cases. Obviously, apart from the soil and wall characteristics, k depends on the geometry of the problem (please notice that both curves make a "step" at z=6 m) and the type of movement (combination of bending, translation and rotation). Structural elements such as struts, also largely affects k.

Finally, the effect of wall roughness was examined numerically. Solving the same embedded wall with, this time, "interface coefficient" equal to 1 (meaning rough wall), no influence is observed on the earth pressures on the active "side" of the problem; on the other hand, there is influence on the earth pressures on the passive "side" (see Figure 11). This outcome is rather logical and expected as on the active "side" the material loosens (gaining volume), reminding nothing of the rigid active wedge of Coulomb's [11] theory. It seems, however, that the assumption of a rigid body wedge is more relevant to the passive state, but in every case, we are in the safe side considering that the wall surface is smooth.

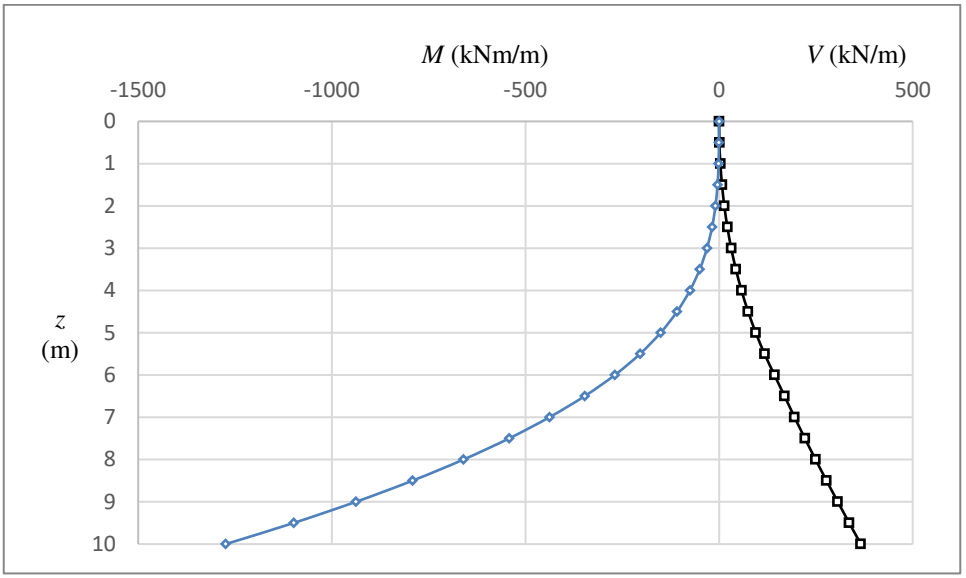

317
318 *Figure 9. Moment and shear force diagram for the "only bending" (no wall translation or rotation) case.*

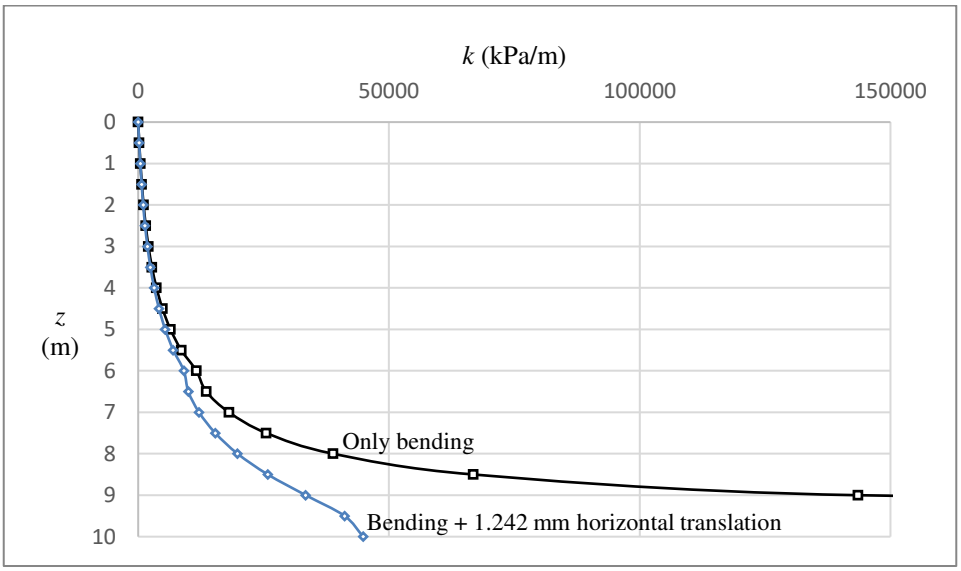

319
320 *Figure 10. Modulus of horizontal subgrade reaction, k, against depth chart.*

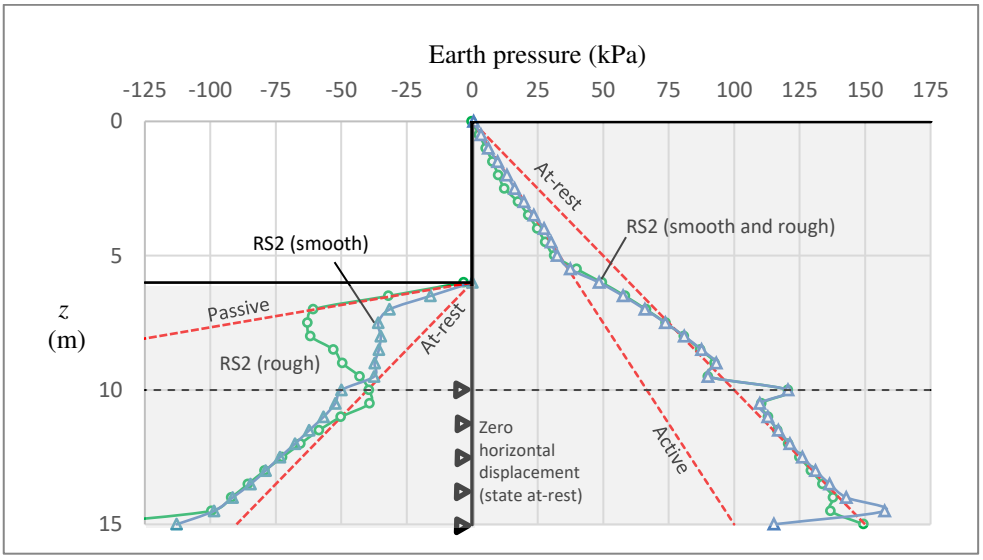

Figure 11. Effect of wall roughness on earth pressures.

4 Conclusions

Intermediate values of earth pressure occur if the wall movements are insufficient to mobilize the active or passive limiting values. These values are of particular importance for designing embedded retaining walls, due to the flexible nature of the latter. The simplistic and empirical methods included in EN1997-1:2004 and prEN1997-3:2022 are far from being considered reliable. In the present paper a new, fully analytical method for designing embedded retaining walls is suggested. This combines the earth pressure method proposed in 2019 by the author with the elastic beam theory.

An application example is given, indicating remarkable agreement with the finite element method. The effectiveness of the proposed method refers not only to the calculation of the earth pressures but also to the calculation of the deflection profile of the wall. Indeed, a great advantage of the proposed method against finite elements is the stability of the results. For the passive state, not only the numerical earth pressure results are very unstable but also they cannot be justified by the deformation characteristics of the wall.

In addition to bending, the proposed method is able to calculate the final deformation of the wall (and apparently, the respective earth pressures), which may include translational movement and/or rotation around a pivot point; the latter lies somewhere between the free soil surface on the passive side and the lower end of the wall, but not at the latter. The wall, which

floats in the soil, will find its final position satisfying simultaneously the *equilibrium of the energy* and the *principle of least action.*

With the earth pressures on both sides of the wall being reliably calculated, the bending moments and shear forces are also possible to be calculated fully analytically. In addition to this, the horizontal coefficient of subgrade reaction, k, along the wall can be back-calculated by the intermediate earth pressure and deflection charts. As shown, k largely depends on the geometry of the problem (including the presence of any structural element, such as struts) and the type of movement (combination of bending, translation and rotation) of the wall. Finally, it has been shown that the wall roughness plays no role in the magnitude of intermediate active earth pressures, while when neglecting it from the calculation of the intermediate passive ones, we are on the safe side.

Appendix A: Analytical procedure for calculating the mobilized shear strength parameters

The analytical solution of Equation 3 is the following expression:

$$\varphi_m = Re\left(\sin^{-1}\left(-\frac{b_o+\frac{D_0}{C_0\zeta^{\lambda}}+C_0\zeta^{\lambda}}{3a_o}\right)\right)\frac{180}{\pi}\ (^{o}) \tag{14}$$

where, $a_o = (2\lambda-1)(1+e_2^2\tan^2\varphi')$, $b_o = 1-(2\,e_1e_2+e_2^2)\tan^2\varphi'$, $c_o = (2\lambda-1)(e_1^2+2\,e_1e_2)\tan^2\varphi'$, $d_o = -e_1^2\tan^2\varphi'$, $D_0 = b_o^2-3a_o\,c_o$, $D_1 = 2b_o^3-9\,a_o\,b_o\,c_o+27a_o^2\,d_o$, $C_0 = \sqrt[3]{\frac{1}{2}\left(D_1-\sqrt{D_1^2-4D_0^3}\right)}$, $e_1 = |1-A_0|/B_1$, $e_2 = C_1/B_1$ and $\zeta = -\frac{1}{2}+\frac{\sqrt{3}}{2}i$. The Re notation means that only the real part of the number is kept; the imaginary part is infinitesimally small, and thus, practically zero.

- For the active "side" of the problem (any soil state between the state at-rest and the active state), $\lambda = 1$. Also,

$$A_0 = \frac{1-\sin\varphi'}{1+\sin\varphi'}\left(1-\xi\,\sin\varphi'+\tan\theta_{eq}\tan\varphi'\left(2+\xi(\,1-\,\sin\varphi')\right)\right) \tag{15}$$

$$B_1 = \frac{2c'}{(1-a_v)(\sigma_v-u)}\tan\left(\frac{\pi}{4}-\frac{\varphi'}{2}\right) \tag{16}$$

- For the passive "side" of the problem (any soil state between the state at-rest and the passive state), $\lambda = 0$ when $K_{XE} \geq 1$ and $\lambda = 1$ when $K_{XE} \leq 1$ (try either $\lambda = 0$ or $\lambda = 1$ and check is the respective inequality stands; if not, use the other λ value). Also,

$$A_0 = \left(\frac{1+\sin\varphi'}{1-\sin\varphi'}\right)^{\xi_1} \left(1 + \xi \sin\varphi' + \xi_2 \tan\theta_{eq} \tan\varphi' \left(2 + \xi \left(1 + \sin\varphi'\right)\right)\right) \quad (17)$$

$$B_1 = \frac{2c\prime}{(1-a_v)\,(\sigma_v - u)} \tan\left(\frac{\pi}{4} - \frac{\varphi\prime}{2}\right) \left(\frac{\tan\left(\frac{\pi}{4}+\frac{\varphi\prime}{2}\right)}{\tan\left(\frac{\pi}{4}-\frac{\varphi\prime}{2}\right)}\right)^{\xi_1} \quad (18)$$

- For both the active and the passive "side" of the problem:

$$C_1 = \frac{2c\prime}{(1-a_v)\,(\sigma_v - u)\tan\varphi\prime} + 1 + A_0 \quad (19)$$

Appendix B: Effectiveness of m factor

The effectiveness of the m factor is illustrated herein using an example where a rigid wall is translated towards the passive state in 11 steps, that is from $\Delta x/\Delta x_{max}$ = 0 (state at-rest) to 1 (passive state) with 0.1 interval. The wall is 3-meter tall and it is pushed towards a soil with c'=0 kPa, φ'=25° and γ=20 kN/m^3; the system is subjected to a horizontal sesimic excitation with a_h=0.2 (the vertical pseudo-static coefficient, a_v, is zero). The numerical resuts have been obtained using Rocscience's RS2; avoiding repeatition, the full desciption of the finite element procedure followed is described in Pantelidis and Christodoulou [8]. As shown in Figure 12, there is an excellent agreement between the analytical results of the proposed method and the respective numerical ones, at least upto the depth near the lower end of the wall; near the lower end, the numerical passive earth pressures appears bloated.

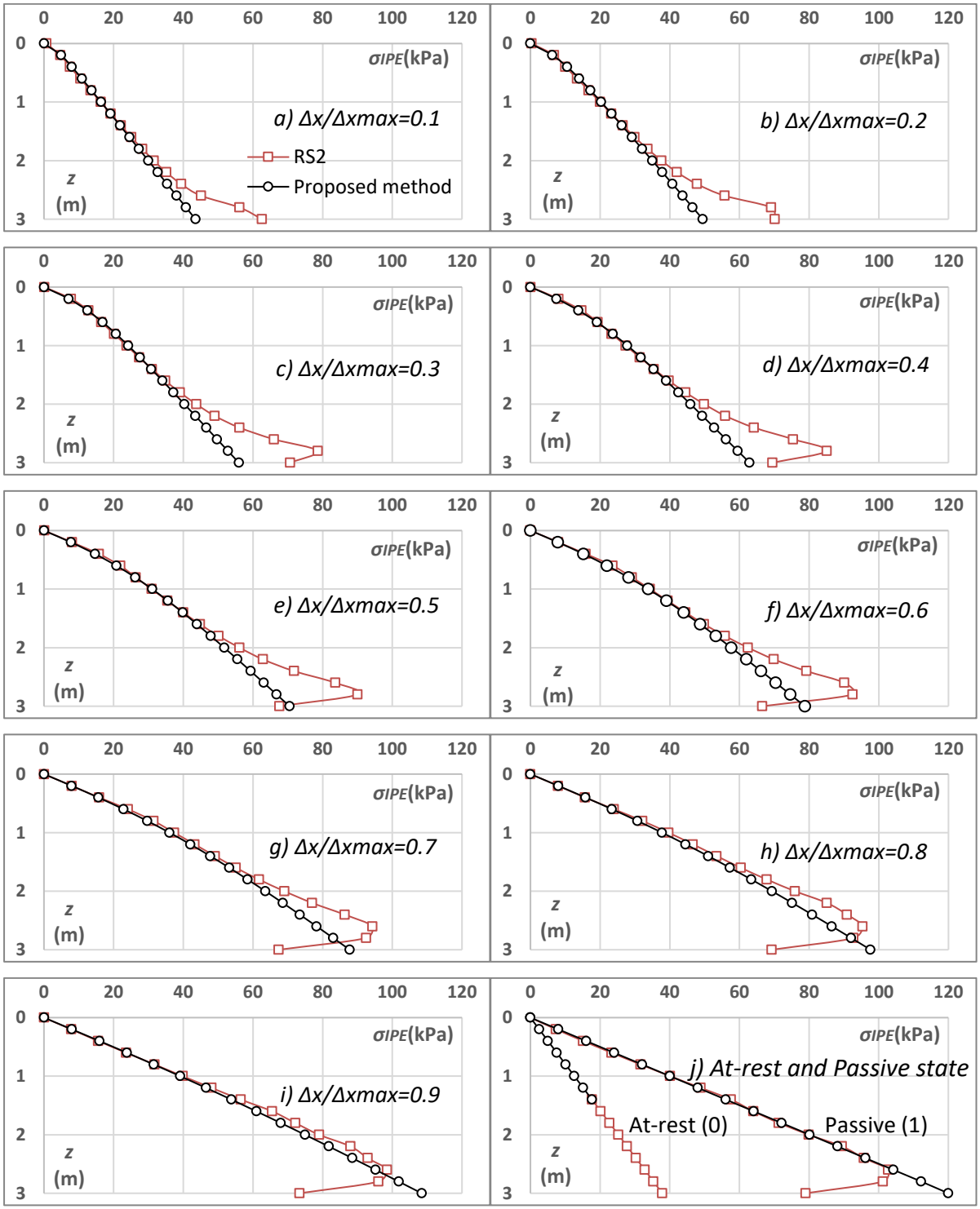

Figure 12. Charts showing the effectiveness of the m factor for $\Delta x/\Delta x_{max}$ = 0 (state at-rest) to 1 (passive state) with 0.1 interval.

Appendix C: Calculating Δx for the case of cantilever beam with partially distributed linearly varying load (trapezoidal) based on the elastic beam theory

$$\Delta x = \begin{cases} -\frac{R_A x^3}{6EI} - \frac{M_A x^2}{2EI}, x \le a \\ -\frac{R_A x^3}{6EI} - \frac{M_A x^2}{2EI} + \frac{(4W_1+W_x)x_a^4}{120EI}, a < x < L-b \\ -\frac{R_A L_b^3}{6EI} - \frac{M_A L_b^2}{2EI} + \frac{(4W_1+W_2)L_w^4}{120EI} - \theta_B(x-L_b), x \ge L-b \end{cases} \quad (20)$$

where, $R_A = L_w W_m$ (shear forces reaction at point A), $M_A = -\frac{3a+L_w}{3} L_w W_m - \frac{L_w^2}{6} W_2$ (moment reaction at point A), $\theta_B = -L_w \frac{(2a^2+L_1^2)W_m + L_1 L_w W_2}{12EI}$ (slope of beam at point B), $x_a = x - a$, $L_w = L - a - b$, $L_1 = L + a - b$, $L_b = L - b$, $W_m = \frac{W_1+W_2}{2}$ and $W_x = W_1 + \frac{W_2 - W_1}{L_w}(x-a)$. The notation shown in Figure 13 is used. x is measured from point A. The equations have been copied from [12].

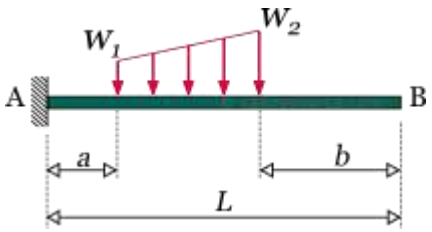

Figure 13. Partially distributed linearly varying load on cantilever beam [12].

Appendix D: Application example - Iterative procedure

Table A1. 1st iteration

Active "side"										Passive "side"									Total
z	$\frac{H_A}{z_A}$	$\Delta x^{(1)}$	$\frac{\Delta_x}{\Delta x_M}$	m	λ	φ_m	$K_{XE}{}^{(2)}$	σ_{XE}	Δ_x	$\frac{H_P}{z_P}$	$\Delta x^{(1)}$	$\frac{\Delta_x}{\Delta x_M}$	m	λ	φ_m	$K_{XE}{}^{(2)}$	σ_{XE}	Δx	Δx_{tot}
(m)		(mm)				(°)		(kPa)	(mm)		(mm)				(°)		(kPa)	(mm)	(mm)
0	∞	0	0	1	1	19.471	0.500	0.00	22.22									0.62	21.60
0.5	20.00	0	0	1	1	19.471	0.500	5.00	20.83									0.58	20.25
1	10.00	0	0	1	1	19.471	0.500	10.00	19.44									0.55	18.90
1.5	6.67	0	0	1	1	19.471	0.500	15.00	18.05									0.51	17.54
2	5.00	0	0	1	1	19.471	0.500	20.00	16.67									0.48	16.19
2.5	4.00	0	0	1	1	19.471	0.500	25.00	15.28									0.44	14.84
3	3.33	0	0	1	1	19.471	0.500	30.00	13.90									0.41	13.50
3.5	2.86	0	0	1	1	19.471	0.500	35.00	12.53									0.37	12.16
4	2.50	0	0	1	1	19.471	0.500	40.00	11.17									0.33	10.83
4.5	2.22	0	0	1	1	19.471	0.500	45.00	9.82									0.30	9.53
5	2.00	0	0	1	1	19.471	0.500	50.00	8.51									0.26	8.24
5.5	1.82	0	0	1	1	19.471	0.500	55.00	7.22									0.23	7.00
6	1.67	0	0	1	1	19.471	0.500	60.00	5.99	∞	0	0	1	1	19.471	0.500	0.00	0.19	5.80
6.5	1.54	0	0	1	1	19.471	0.500	65.00	4.81	8	0	0	1	1	19.471	0.500	5.00	0.16	4.65
7	1.43	0	0	1	1	19.471	0.500	70.00	3.71	4	0	0	1	1	19.471	0.500	10.00	0.12	3.59
7.5	1.33	0	0	1	1	19.471	0.500	75.00	2.71	2.67	0	0	1	1	19.471	0.500	15.00	0.09	2.62
8	1.25	0	0	1	1	19.471	0.500	80.00	1.82	2.00	0	0	1	1	19.471	0.500	20.00	0.06	1.77
8.5	1.18	0	0	1	1	19.471	0.500	85.00	1.08	1.60	0	0	1	1	19.471	0.500	25.00	0.03	1.05
9	1.11	0	0	1	1	19.471	0.500	90.00	0.50	1.33	0	0	1	1	19.471	0.500	30.00	0.01	0.49
9.5	1.05	0	0	1	1	19.471	0.500	95.00	0.13	1.14	0	0	1	1	19.471	0.500	35.00	0.00	0.13
10	1.00	0	0	1	1	19.471	0.500	100.00	0.00	1.00	0	0	1	1	19.471	0.500	40.00	0.00	0.00

(1) $\Delta_x = 0$ mm (initial value)

(2) $K_{XE} = K_{OE}$ (initial value standing for $\Delta_x = 0$ mm)

Table A2. 2nd iteration

Active "side"										Passive "side"									Total
z	$\frac{H_A}{z_A}$	$\Delta x^{(1)}$	$\frac{\Delta_x}{\Delta x_M}$	m	λ	φ_m	K_{XE}	σ_{XE}	Δ_x	$\frac{H_P}{z_P}$	$\Delta x^{(1)}$	$\frac{\Delta_x}{\Delta x_M}$	m	λ	φ_m	K_{XE}	σ_{XE}	Δx	Δx_{tot}
(m)		(mm)				(°)		(kPa)	(mm)		(mm)				(°)		(kPa)	(mm)	(mm)
0	∞	21.60	1.000	∞	1	30.000	0.333	0.00	17.28									0.81	16.47
0.5	20.00	20.25	1.000	$4 \cdot 10^7$	1	30.000	0.333	3.33	16.21									0.76	15.45
1	10.00	18.90	0.940	1381	1	29.982	0.334	6.67	15.14									0.71	14.43
1.5	6.67	17.54	0.873	247.2	1	29.900	0.335	10.04	14.07									0.67	13.41
2	5.00	16.19	0.805	80.8	1	29.698	0.337	13.49	13.00									0.62	12.38
2.5	4.00	14.84	0.738	35.2	1	29.322	0.343	17.12	11.94									0.57	11.36
3	3.33	13.50	0.671	18.3	1	28.741	0.351	21.03	10.87									0.53	10.35
3.5	2.86	12.16	0.605	10.7	1	27.959	0.362	25.31	9.81									0.48	9.33
4	2.50	10.83	0.539	6.957	1	27.020	0.375	30.02	8.76									0.43	8.33
4.5	2.22	9.53	0.474	4.823	1	25.992	0.391	35.15	7.73									0.39	7.34
5	2.00	8.24	0.410	3.543	1	24.945	0.407	40.67	6.70									0.34	6.36
5.5	1.82	7.00	0.348	2.729	1	23.938	0.423	46.50	5.71									0.29	5.41
6	1.67	5.80	0.288	2.187	1	23.011	0.438	52.55	4.74	∞	5.80	0.120	1.137	1	12.215	0.348	0.00	0.25	4.50
6.5	1.54	4.65	0.232	1.814	1	22.185	0.452	58.73	3.82	8	4.65	0.096	2.151	1	0.554	0.981	9.81	0.20	3.62
7	1.43	3.59	0.179	1.548	1	21.469	0.464	64.98	2.96	4	3.59	0.074	1.437	1	9.446	0.718	14.36	0.15	2.81
7.5	1.33	2.62	0.130	1.357	1	20.865	0.475	71.21	2.17	2.67	2.62	0.054	1.219	1	13.917	0.612	18.37	0.11	2.06
8	1.25	1.77	0.088	1.219	1	20.372	0.484	77.37	1.46	2.00	1.77	0.037	1.116	1	16.378	0.560	22.40	0.07	1.39
8.5	1.18	1.05	0.052	1.120	1	19.986	0.491	83.39	0.87	1.60	1.05	0.022	1.058	1	17.873	0.530	26.51	0.03	0.83
9	1.11	0.49	0.025	1.053	1	19.706	0.496	89.22	0.41	1.33	0.49	0.010	1.024	1	18.793	0.513	30.76	0.01	0.40
9.5	1.05	0.13	0.007	1.014	1	19.532	0.499	94.78	0.11	1.14	0.13	0.003	1.006	1	19.305	0.503	35.21	0.00	0.11
10	1.00	0.00	0.000	1.000	1	19.471	0.500	100.00	0.00	1.00	0.00	0.000	1.000	1	19.471	0.500	40.00	0.00	0.00

(1) These are the Δx_{tot} values taken from the previous table.

Table A3. 3rd iteration

Active "side"										Passive "side"									Total
z	$\frac{H_A}{z_A}$	$\Delta x^{(1)}$	$\frac{\Delta_x}{\Delta x_M}$	m	λ	φ_m	$K_{XE}{}^{(2)}$	σ_{XE}	Δ_x	$\frac{H_P}{z_P}$	$\Delta x^{(1)}$	$\frac{\Delta_x}{\Delta x_M}$	m	λ	φ_m	$K_{XE}{}^{(2)}$	σ_{XE}	Δx	Δx_{tot}
(m)		(mm)				(°)		(kPa)	(mm)		(mm)				(°)		(kPa)	(mm)	(mm)
0	∞	16.47	0.819	∞	1	30.000	0.333	0.00	17.88									0.77	17.11
0.5	20.00	15.45	0.769	668.8	1	29.963	0.334	3.34	16.77									0.72	16.05
1	10.00	14.43	0.718	136.3	1	29.820	0.336	6.71	15.67									0.68	14.99
1.5	6.67	13.41	0.667	50.2	1	29.520	0.340	10.19	14.56									0.64	13.92
2	5.00	12.38	0.616	24.2	1	29.031	0.347	13.86	13.45									0.59	12.86
2.5	4.00	11.36	0.565	13.6	1	28.353	0.356	17.80	12.35									0.55	11.80
3	3.33	10.35	0.515	8.630	1	27.519	0.368	22.08	11.25									0.50	10.75
3.5	2.86	9.33	0.464	5.899	1	26.586	0.382	26.71	10.15									0.46	9.70
4	2.50	8.33	0.414	4.294	1	25.617	0.396	31.70	9.07									0.41	8.65
4.5	2.22	7.34	0.365	3.285	1	24.665	0.411	37.00	7.99									0.37	7.62
5	2.00	6.36	0.317	2.617	1	23.767	0.425	42.55	6.93									0.32	6.61
5.5	1.82	5.41	0.269	2.156	1	22.948	0.439	48.28	5.90									0.28	5.62
6	1.67	4.50	0.224	1.827	1	22.217	0.451	54.15	4.90	∞	4.50	0.093	∞	1	12.214	0.348	0.00	0.24	4.67
6.5	1.54	3.62	0.180	1.586	1	21.577	0.462	60.09	3.95	8	3.62	0.075	1.840	1	3.117	0.897	8.97	0.19	3.76
7	1.43	2.81	0.140	1.406	1	21.026	0.472	66.06	3.06	4	2.81	0.058	1.329	1	11.539	0.667	13.33	0.15	2.91
7.5	1.33	2.06	0.102	1.270	1	20.562	0.480	72.02	2.24	2.67	2.06	0.043	1.168	1	15.094	0.587	17.60	0.11	2.13
8	1.25	1.39	0.069	1.169	1	20.180	0.487	77.92	1.51	2.00	1.39	0.029	1.090	1	17.026	0.547	21.88	0.07	1.44
8.5	1.18	0.83	0.041	1.095	1	19.880	0.492	83.72	0.90	1.60	0.83	0.017	1.046	1	18.200	0.524	26.20	0.03	0.86
9	1.11	0.40	0.020	1.043	1	19.660	0.497	89.37	0.42	1.33	0.40	0.008	1.019	1	18.926	0.510	30.61	0.01	0.41
9.5	1.05	0.11	0.005	1.011	1	19.521	0.499	94.82	0.11	1.14	0.11	0.002	1.005	1	19.336	0.503	35.18	0.00	0.11
10	1.00	0.00	0.000	1.000	1	19.471	0.500	100.00	0.00	1.00	0.00	0.000	1.000	1	19.471	0.500	40.00	0.00	0.00

(1) These are the Δx_{tot} values taken from the previous table.

Table A4. 4th iteration

	Active "side"									Passive "side"								Total
z	$\frac{H_A}{z_A}$	$\Delta x^{(1)}$	$\frac{\Delta_x}{\Delta x_M}$	m	λ	φ_m	$K_{XE}{}^{(2)}$	σ_{XE}	Δ_x	$\frac{H_P}{z_P}$	$\Delta x^{(1)}$	$\frac{\Delta_x}{\Delta x_M}$	m	λ	φ_m	$K_{XE}{}^{(2)}$	σ_{XE}	Δx	Δx_{tot}
(m)		(mm)				(°)		(kPa)	(mm)		(mm)				(°)		(kPa)	(mm)	(mm)
0	∞	17.11	0.851	∞	1	30.000	0.333	0.00	17.79									0.77	17.02
0.5	20.00	16.05	0.798	871.2	1	29.972	0.334	3.34	16.69									0.73	15.96
1	10.00	14.99	0.746	167.0	1	29.853	0.335	6.70	15.59									0.69	14.91
1.5	6.67	13.92	0.693	59.2	1	29.590	0.339	10.16	14.49									0.64	13.85
2	5.00	12.86	0.640	27.7	1	29.146	0.345	13.80	13.39									0.60	12.79
2.5	4.00	11.80	0.587	15.3	1	28.509	0.354	17.69	12.29									0.55	11.74
3	3.33	10.75	0.535	9.438	1	27.705	0.365	21.91	11.19									0.51	10.69
3.5	2.86	9.70	0.482	6.348	1	26.785	0.379	26.51	10.10									0.46	9.64
4	2.50	8.65	0.430	4.558	1	25.813	0.393	31.46	9.02									0.42	8.61
4.5	2.22	7.62	0.379	3.448	1	24.845	0.408	36.74	7.95									0.37	7.58
5	2.00	6.61	0.329	2.720	1	23.925	0.423	42.29	6.90									0.33	6.57
5.5	1.82	5.62	0.280	2.223	1	23.080	0.437	48.04	5.87									0.28	5.59
6	1.67	4.67	0.232	1.870	1	22.322	0.449	53.93	4.88	∞	4.67	0.097	∞	1	12.214	0.348	0.000	0.24	4.64
6.5	1.54	3.76	0.187	1.614	1	21.658	0.461	59.91	3.93	8	3.76	0.078	1.880	1	2.603	0.913	9.131	0.19	3.74
7	1.43	2.91	0.145	1.424	1	21.085	0.471	65.92	3.04	4	2.91	0.060	1.343	1	11.254	0.673	13.467	0.15	2.90
7.5	1.33	2.13	0.106	1.282	1	20.603	0.479	71.91	2.23	2.67	2.13	0.044	1.175	1	14.935	0.590	17.704	0.11	2.12
8	1.25	1.44	0.072	1.176	1	20.206	0.487	77.85	1.50	2.00	1.44	0.030	1.094	1	16.938	0.549	21.950	0.07	1.44
8.5	1.18	0.86	0.043	1.098	1	19.894	0.492	83.68	0.89	1.60	0.86	0.018	1.048	1	18.155	0.525	26.242	0.03	0.86
9	1.11	0.41	0.020	1.044	1	19.666	0.496	89.35	0.42	1.33	0.41	0.009	1.020	1	18.908	0.510	30.630	0.01	0.41
9.5	1.05	0.11	0.006	1.011	1	19.522	0.499	94.82	0.11	1.14	0.11	0.002	1.005	1	19.331	0.503	35.180	0.00	0.11
10	1.00	0.00	0.000	1.000	1	19.471	0.500	100.00	0.00	1.00	0.00	0.000	1.000	1	19.471	0.500	39.999	0.00	0.00

(1) These are the Δx_{tot} values taken from the previous table.

Table A5. 5th iteration

	Active "side"									Passive "side"								Total
z	$\frac{H_A}{z_A}$	$\Delta x^{(1)}$	$\frac{\Delta_x}{\Delta x_M}$	m	λ	φ_m	$K_{XE}{}^{(2)}$	σ_{XE}	Δ_x	$\frac{H_P}{z_P}$	$\Delta x^{(1)}$	$\frac{\Delta_x}{\Delta x_M}$	m	λ	φ_m	$K_{XE}{}^{(2)}$	σ_{XE}	Δx	Δx_{tot}
(m)		(mm)				(°)		(kPa)	(mm)		(mm)				(°)		(kPa)	(mm)	(mm)
0	∞	17.02	0.847	∞	1	30.000	0.333	0.00	17.80									0.77	17.03
0.5	20.00	15.96	0.794	837.14	1	29.970	0.334	3.34	16.70									0.73	15.97
1	10.00	14.91	0.741	162.05	1	29.848	0.335	6.71	15.60									0.68	14.92
1.5	6.67	13.85	0.689	57.778	1	29.581	0.339	10.17	14.50									0.64	13.86
2	5.00	12.79	0.636	27.129	1	29.130	0.345	13.81	13.40									0.60	12.80
2.5	4.00	11.74	0.584	15.022	1	28.487	0.354	17.71	12.30									0.55	11.75
3	3.33	10.69	0.532	9.315	1	27.678	0.366	21.94	11.20									0.51	10.70
3.5	2.86	9.64	0.480	6.280	1	26.757	0.379	26.54	10.11									0.46	9.65
4	2.50	8.61	0.428	4.518	1	25.785	0.394	31.50	9.03									0.42	8.61
4.5	2.22	7.58	0.377	3.423	1	24.819	0.409	36.78	7.96									0.37	7.59
5	2.00	6.57	0.327	2.705	1	23.902	0.423	42.33	6.91									0.33	6.58
5.5	1.82	5.59	0.278	2.213	1	23.061	0.437	48.08	5.88									0.28	5.60
6	1.67	4.64	0.231	1.864	1	22.307	0.450	53.97	4.88	∞	4.64	0.096	∞	1	12.214	0.348	0.00	0.24	4.65
6.5	1.54	3.74	0.186	1.610	1	21.646	0.461	59.94	3.94	8	3.74	0.078	1.874	1	2.679	0.911	9.11	0.19	3.74
7	1.43	2.90	0.144	1.421	1	21.077	0.471	65.94	3.05	4	2.90	0.060	1.341	1	11.296	0.672	13.45	0.15	2.90
7.5	1.33	2.12	0.106	1.280	1	20.597	0.480	71.93	2.23	2.67	2.12	0.044	1.174	1	14.958	0.590	17.69	0.11	2.12
8	1.25	1.44	0.071	1.175	1	20.203	0.487	77.86	1.50	2.00	1.44	0.030	1.093	1	16.951	0.548	21.94	0.07	1.44
8.5	1.18	0.86	0.043	1.097	1	19.892	0.492	83.68	0.89	1.60	0.86	0.018	1.047	1	18.162	0.525	26.24	0.03	0.86
9	1.11	0.41	0.020	1.044	1	19.665	0.496	89.35	0.42	1.33	0.41	0.008	1.020	1	18.911	0.510	30.63	0.01	0.41
9.5	1.05	0.11	0.005	1.011	1	19.522	0.499	94.82	0.11	1.14	0.11	0.002	1.005	1	19.332	0.503	35.18	0.00	0.11
10	1.00	0.00	0.000	1.000	1	19.471	0.500	100.00	0.00	1.00	0.00	0.000	1.000	1	19.471	0.500	40.00	0.00	0.00

(1) These are the Δx_{tot} values taken from the previous table.

Notation

$a = \Delta x/\Delta x_{max}$

a_b= an empirical backfill-dependent coefficient

a_h= the seismic coefficient of horizontal acceleration

a_v= the seismic coefficient of vertical acceleration (if negative, the vertical pseudo-static force acts downwards, i.e. it increases the unit weight of soil, $(1 + k_v)\gamma$)

γ= the unit weight of soil

$\Delta K = K_{OE} - K_{AE}$ or $K_{PE} - K_{OE}$

Δx = the wall displacement

Δx_{max}= the lateral displacement of wall corresponding to the active or passive state; the symbols $\Delta x_{max,A}$ and $\Delta x_{max,P}$ are also used for the active and passive state respectively

Δx_M = the required horizontal displacement for the development of the active or passive state at the mid-height of the retained soil

$\theta_{eq} = atan\left(\frac{a_H}{1-a_V}\right)$ in the absence of pore water pressure or $atan\left(\frac{a_H}{1-a_V}\frac{\sigma_v}{\sigma_v-u}\right)$ in the presence of pore water pressure

λ = a soil state dependent coefficient being either 0 or 1

ν = the Poisson's ratio of the retained soil

$\xi = (m-1)/(m+1) - 1.$

$\xi_1 = 1 + \xi$ (parameter related to the transition from the soil wedge of the state at-rest to the soil wedge of the passive state)

$\xi_2 = 2/m - 1$ (as ξ_1)

σ_{AE}, σ_{PE} or σ_{OE} = the active, passive or at-rest earth pressure in the seismic situation

σ_v= the vertical total stress

φ'= the effective internal friction angle of soil

φ_m= the mobilized friction angle of soil

c'= the effective cohesion of soil

c_m= the mobilized cohesion of soil

D = the embedment depth

d = the interaction length

457 E = the elastic modulus of the retained soil

458 E_s= the secant soil's modulus of elasticity

459 E_w=Young's modulus of the embedded wall

460 H= the height of the retained soil on the active or the passive "side" of the problem (H_A and
461 H_P respectively)

462 h = the height of the retaining wall

463 I_w= moment of inertia of the embedded wall

464 K_A =Rankine's coefficient of active earth pressure

465 Ko = Jaky's (static) coefficient of earth pressure at-rest

466 K_{AE}, K_{PE} or K_{OE} = the active, passive or at-rest coefficients of earth pressure in the seismic
467 situation

468 $K_{\mathrm{ph,mob}}$ = mobilized passive earth pressure coefficient

469 K_{ph} = the horizontal component of the coefficient of passive earth pressure

470 k= the horizontal modulus of subgrade reaction of soil

471 m=real positive number ranging from 1 to $+\infty$

472 P_{AE}, P_{PE} or P_{OE} = the active, passive or at-rest resultant earth pressure force in the seismic
473 situation

474 s_h = the horizontal displacement at the wall top

475 $v(z)$ = the horizontal displacement at depth z

476 u = the pore water pressure

477 z= the depth where the earth pressure is calculated

478 **Data availability statement**

479 All data generated or used during the study are available from the corresponding author by
480 request.

Declaration of Competing Interest

The author declare that they have no known competing financial interests or personal relationships that could have appeared to influence the work reported in this paper.

References

1. EN1997-1 (2004) Eurocode 7: Geotechnical design, Part 1: General rules. European Committee for Standarization, Brussels
2. prEN1997-3:2022 (2022) Eurocode 7 - Geotechnical design - Part 3: Geotechnical structures (draft standard)
3. Pantelidis L (2019) The Generalized Coefficients of Earth Pressure: A Unified Approach. Appl Sci 9:5291
4. Rankine WJM (1857) II. On the stability of loose earth. Philos Trans R Soc London 9–27
5. EN1998-5:2004 (2004) Eurocode 8 - Design of structures for earthquake resistance - Part 5: Geotechnical aspects, foundations, retaining walls and underground structures
6. prEN1998-5:2022 (2022) Eurocode 8 - Earthquake resistance design of structures - Part 5: Geotechnical aspects, foundations, retaining walls and underground structures (draft standard)
7. AASHTO (2007) AASHTO LRFD bridge design specifications. Transp (Amst) Am Assoc State Highw Transp Off Inc Washington, DC 1635. https://doi.org/10.1111/febs.12237
8. Pantelidis L, Christodoulou P (2022) Comparing Eurocode 8-5 and AASHTO methods for earth pressure analysis against centrifuge tests, finite elements, and the Generalized Coefficients of Earth Pressure. ResearchSquare (preprint): https://doi.org/10.21203/rs.3.rs-1808466/v2
9. Pantelidis L (2022) Shaft resistance capacity of axially loaded piles in cohesive-frictional soils under static or pseudo-static conditions based on ground parameters. ResearchSquare (preprint): https://doi.org/10.21203/rs.3.rs-1986330/v1
10. Rocscience Inc. (2022) RS2: Joints.

https://www.rocscience.com/help/rs2/documentation/knowledge-base/joints. Accessed 9 Jun 2022

11. Coulomb CA (1776) An attempt to apply the rules of maxima and minima to several problems of stability related to architecture. Mémoires l'Académie R des Sci 7:343–382

12. Lemonis M (2022) CALC RESOURCE. https://calcresource.com/statics-cantilever-beam.html